HHS Public Access

Author manuscript

Neuron. Author manuscript; available in PMC 2016 January 07.

Published in final edited form as:

Neuron. 2015 January 7; 85(1): 190–201. doi:10.1016/j.neuron.2014.12.001.

Hippocampal CA2 activity patterns change over time to a larger extent than between spatial contexts

Emily A. Mankin[1], **Geoffrey W. Diehl**[1], **Fraser T. Sparks**[2,4], **Stefan Leutgeb**[1,3], and **Jill K. Leutgeb**[1,*]

[1]Neurobiology Section and Center for Neural Circuits and Behavior, Division of Biological Sciences, University of California, San Diego, La Jolla, CA 92093, USA

[2]Canadian Centre for Behavioural Neuroscience, Department of Neuroscience, University of Lethbridge, Lethbridge, AB T1K 3M4, Canada

[3]Kavli Institute for Brain and Mind, University of California, San Diego, La Jolla, CA 92093, USA

Summary

The hippocampal CA2 subregion has a different anatomical connectivity pattern within the entorhino-hippocampal circuit than either the CA1 or CA3 subregion. Yet major differences in the neuronal activity patterns of CA2 compared to the other CA subregions have not been reported. We show that standard spatial and temporal firing patterns of individual hippocampal principal neurons in behaving rats, such as place fields, theta modulation, and phase precession, are also present in CA2, but that the CA2 subregion differs substantially from the other CA subregions in its population coding. CA2 ensembles do not show a persistent code for space or for differences in context. Rather, CA2 activity patterns become progressively dissimilar over time periods of hours to days. The weak coding for a particular context is consistent with recent behavioral evidence that CA2 circuits preferentially support social, emotional, and temporal rather than spatial aspects of memory.

Introduction

The hippocampal CA fields are subdivided into the CA3, CA2, and CA1 subregions based on unique cytoarchitecture, connectivity, physiology, and gene expression patterns (Kjonigsen et al., 2011; Lein et al., 2005; Lorente de No, 1934; Woodhams et al., 1993; Zhao et al., 2001). Standard circuit diagrams of the hippocampal formation include a trisynaptic loop from the entorhinal cortex to the dentate gyrus, from the dentate gyrus to CA3, and from CA3 to CA1, as well as additional direct connections from entorhinal cortex to the dentate gyrus, the CA3 subregion, and the CA1 subregion. Although it has long been recognized that the hippocampal CA2 subregion is distinct from the other CA subregions in

* Correspondence: jleutgeb@ucsd.edu.

[4]Present address: Center for Neural Science, New York University, New York, NY 10003, USA

that it receives inputs from the supramammillary nucleus (Cui et al., 2013; Jones and McHugh, 2011; Magloczky et al., 1994; Pan and McNaughton, 2004; Woodhams et al., 1993), it has primarily been considered as a transition zone between CA1 and CA3. However, major differences from CA3 and CA1 in CA2 connectivity within the hippocampal circuit and with entorhinal cortex have recently been described (Cui et al., 2013; Hitti and Siegelbaum, 2014; Kohara et al., 2014; Rowland et al., 2013). Notably, CA2 neurons are strongly excited by distal dendritic inputs from the entorhinal cortex and only weakly activated by CA3 inputs (Bartesaghi and Gessi, 2004; Bartesaghi et al., 2006; Chevaleyre and Siegelbaum, 2010; Kohara et al., 2014; Zhao et al., 2007). Thus, entorhinal information arrives in CA1 via the CA2 pathway in parallel to the direct pathway to CA1 and the indirect pathway through the dentate/CA3 subregions (Figure 1A).

In addition to these major differences in connectivity, CA2 is unique among hippocampal subregions in its mechanisms for long-term plasticity and in the baseline membrane properties of its principal cells (Caruana et al., 2012; Chevaleyre and Siegelbaum, 2010; Jones and McHugh, 2011; Pagani et al., 2014; Zhao et al., 2007). Furthermore, behavioral studies support a potentially unique functional role for CA2 in memory by demonstrating that the vasopressin 1b receptor, which is selectively enriched in CA2 neurons (Young et al., 2006), is necessary for social recognition and for discriminating the recency of an event (DeVito et al., 2009; Wersinger et al., 2002). In addition, CA2 has been directly found to be necessary for aggression towards intruders and for social memory (Hitti and Siegelbaum, 2014; Pagani et al., 2014). Neither vasopression 1b receptor knockout nor genetic silencing of CA2, however, affects spatial or contextual memory (Wersinger et al., 2002; Hitti and Siegelbaum, 2014; DeVito et al., 2009).

Major differences in anatomical and functional characteristics between hippocampal subregions do not *a priori* enable predictions of whether or how neural network firing patterns will differ in behaving animals. For example, standard spatial and temporal firing patterns of hippocampal principal cells, such as place fields, theta modulation, and phase precession, are remarkably similar between CA1 and CA3, despite the substantial differences in connectivity and function between these subregions. Differences in neuronal activity patterns between these subregions only become apparent when considering how activity across the entire population of neurons responds to different behavioral situations. For example, when conflicting cues are presented, CA1 cells show a heterogeneous response, with different subpopulations responding to each aspect of an environment or memory task, while the cell population in the CA3 subregion more coherently follows one set of cues (Lee et al., 2004; Leutgeb et al., 2007; Leutgeb et al., 2004; Vazdarjanova and Guzowski, 2004). Additionally, firing patterns change over time in the CA1 population (Ludvig, 1999; Mankin et al., 2012; Manns et al., 2007; Ziv et al., 2013) while they remain more consistent within the CA3 network (Mankin et al., 2012). These differences in population responses indicate that each hippocampal subregion performs specialized computations that, in concert, can support the acquisition and retrieval of the different aspects of episodic memories (Marr, 1971; McNaughton and Morris, 1987; Rolls, 1989; Treves and Rolls, 1994). We thus asked whether the CA2 network might show neuronal coding at the population level that is distinct from CA1 and CA3 and, consistent with

behavioral studies (DeVito et al., 2009; Hitti and Siegelbaum, 2014; Wersinger et al., 2002), may show less specialized network coding for spatial compared to temporal aspects of memories.

Results

To examine how time and contextual change effect firing patterns in CA2, we obtained single unit and local field potential recordings in an experimental design in which rats randomly foraged in highly familiar environments in the morning and again, after an interval of 6 hours, in the afternoon (Figure 1). Each morning and afternoon block consisted of four 10-min sessions, two in a square and two in a circular enclosure, and the enclosure shapes were presented in random order within each testing block. The identity of hippocampal CA2 cells (n = 62 cells in 5 rats) was tracked for a total of sixteen sessions (Figure S1) from the morning block of one recording day through the afternoon block of the next recording day (i.e., 4 recording blocks with 4 sessions each). The recordings from the CA2 region were simultaneous with recordings from tracked CA1 cells (n = 43 in 4 rats) and/or tracked CA3 cells (n = 42 in 3 rats) (see Table S1 for the number of cells per rat). For the comparisons with CA1 and CA3, we also included additional simultaneous recordings from these two subregions in the same experimental design (n = 46 CA1 cells and 29 CA3 cells in 3 rats; Mankin et al., 2012). Recording locations were confirmed using anatomical criteria and immunohistochemical markers specific for CA2 neurons (Figures 1B–C; Figure S2).

We first analyzed the spatial firing patterns of hippocampal cells within each of the sixteen 10-min sessions and, for each cell, averaged across the sixteen sessions. CA2 cells had a higher mean firing rate than either CA1 or CA3 cells (Mann-Whitney *U*: CA1 vs. CA2, $z = -2.96$, $P = 0.0062$; CA1 vs. CA3, $z = 1.51$, $P = 0.13$; CA2 vs. CA3, $z = 3.43$, $P = 0.0018$; see Table S2 and S3 for detailed statistics for all Mann-Whitney *U* tests) (Figure 2A and 2B). However, when considering the peak firing among all spatial locations in the enclosure, there were no differences between subregions (Mann-Whitney *U*: CA1 vs. CA2, $z = -0.30$, $P = 0.77$; CA1 vs. CA3, $z = 2.09$, $P = 0.087$; CA2 vs. CA3, $z = 2.19$, $P = 0.087$) (Figure 2C). A higher mean rate without a difference in peak rate could emerge from broader spatial firing in CA2 compared to the other hippocampal subregions. Consistent with this notion, the amount of spatial information per cell was lower in CA2 compared to CA1 and CA3 (Mann-Whitney *U*: CA1 vs. CA2, $z = 5.85$, $P < 0.001$; CA1 vs. CA3, $z = 0.93$, $P = 0.35$; CA2 vs. CA3, $z = -4.95$, $P < 0.001$) (Figure 2D). We then asked whether the lower spatial information in the CA2 cell population indicated that many of the CA2 cells were somewhat less spatially tuned or whether the lower average may have emerged from a heterogeneous population of CA2 cells in which some cells remained spatially tuned while others had extremely weak spatial tuning. Of the CA2 principal neurons that were active during any of the recorded 10-min sessions (n = 54 of 62), we found that all had a spatial information score that was higher than 0.75 and place fields smaller than 25 % of the recording enclosure in at least one session, which indicates that each cell showed at least moderate spatial tuning.

To further characterize the spatial firing of CA2 cells, we calculated the number of place fields per cell and the size of each place field. The number of place fields per cell was higher in CA2 compared to the other subregions (Mann-Whitney *U*: CA1 vs. CA2, $z = -2.37$, $P =$

0.035; CA1 vs. CA3, $z = 2.30$, $P = 0.035$; CA2 vs. CA3, $z = 3.73$, $P < 0.001$) (Figure 2E). Because many cells in CA1 and CA3 were either silent during behavior and hence did not have a place field or had only one place field during behavior, this resulted in an average of less than one field per cell in CA1 and CA3. To examine whether a higher proportion of active cells per session in CA2 (CA1, 59.2 %; CA2, 68.2 %; CA3, 48.1 %) may have resulted in the larger number of fields, we restricted the analysis to cells that had at least one place field. Even when considering only cells with at least one field, CA2 had more fields per cell than the other hippocampal subregions (Table S2) (Mann-Whitney *U*: CA1 vs CA2, $z = -2.85$, $P = 0.0088$; CA1 vs. CA3, $z = 1.49$, $P = 0.14$; CA2 vs. CA3, $z = 3.28$, $P = 0.0032$). When measuring field size, we found that the fields of CA2 cells were 24.5 % larger than those of CA1 cells (Mann-Whitney *U*: CA1 vs. CA2, $z = -2.54$, $P = 0.034$) (Figure 2F). The difference between CA2 and CA3 did not reach statistical significance (Mann-Whitney *U*: CA2 vs. CA3, $z = 2.2$, $P = 0.053$). The less pronounced difference in field size compared to spatial information can be explained by the fact that the reduction of spatial information in CA2 is caused by the combination of a larger number of fields per neuron and an increase in field size. Because field size in CA2 was moderately larger than in CA1, we considered whether the increased field size in CA2 might be a result of slow spatial drift throughout the 10-min recording session. To examine this possibility, we first calculated field size using spatial maps that were obtained from either the first or the second 5-min half of the session. CA2 had larger fields than either CA1 or CA3 even over 5-min periods (Mann-Whitney *U*: CA1 vs. CA2, $z = -2.31$, $P = 0.042$; CA1 vs. CA3, $z = 1.94$, $P = 0.052$; CA2 vs. CA3, $z = 3.62$, $P < 0.001$). To then directly examine whether fields became larger by drift, we constructed spatial maps from 5 minutes of recording data that were sampled by including either only the odd or only the even minutes of the 10-min recording session. We then compared the field sizes from the continuous 5-min periods with the field size from the interleaved samples over 10 minutes and found no difference (Mann Whitney *U*: CA1, $z = 0.38$, $P = 0.71$; CA2, $z = 0.78$, $P = 0.44$; CA3, $z = -0.64$, $P = 0.52$). This is evidence that spatial drift on a time scale of minutes does not account for the larger fields in CA2.

After confirming that CA2 fields showed no evidence of greater spatial variability within a 10-min recording session than those in CA1 or CA3, we also examined the variability of the firing rates throughout the session. The variability in the firing rates between passes through the field did not differ between CA2 and the other subregions (Mann-Whitney *U*: CA1 vs. CA2, z = 1.90, $P = 0.11$; CA1 vs. CA3, $z = 2.85$, $P = 0.013$; CA2 vs. CA3, $z = 1.20$, $P = 0.23$) (Figure 2G). The standard measurement of variability is not sensitive to a systematic drift in firing rate throughout the 10-min recording session. We therefore estimated by how much the firing rate within each place field changed between the beginning and the end of a 10-min session, and found that the change was smallest in CA2 (Mann-Whitney *U*: CA1 vs. CA2, $z = 3.5$, $P = 0.0016$; CA1 vs. CA3, $z = 0.57$, $P = 0.57$; CA2 vs. CA3, $z = -2.4$, $P = 0.033$). Taken together, we found no evidence that place field location or firing rate in CA2 is less stable than in CA1 or CA3 cells during a single 10-minute random foraging session.

We also examined the relationship between firing in CA2 cells and the hippocampal theta rhythm and found that the depth of theta modulation of CA2 cells was not different from

CA1 and CA3 (Mann-Whitney *U*: CA1 vs. CA2, $z = 0.79$, $P = 0.85$; CA1 vs. CA3, $z = 1.28$, $P = 0.60$; CA2 vs. CA3, $z = 0.65$, $P = 0.85$) and that the intrinsic theta frequency of CA2 cells was not different from CA3 (Mann-Whitney *U*: CA2 vs. CA3, $z = -0.36$, $P = 0.72$) though slower than in CA1 (Mann-Whitney *U*: CA1 vs. CA2, $z = 4.75$, $P < 0.001$). To determine to what extent the phase at which cells fire within the theta cycle precesses during running through the place field, we calculated the slope of the phase-distance relationship for each place field (O'Keefe and Recce, 1993). The slopes of CA2 fields were significantly less than 0 (sign test: n = 53, sign = 4, $P < 0.001$), indicating that the majority of CA2 place cells phase precessed, although the magnitude of the precession was less than in CA1 (Mann-Whitney *U*: CA1 vs. CA2, $z = -4.97$, $P < 0.001$). This difference is consistent with the well-established relation between a larger field size and a less pronounced phase precession (Shen et al., 1997). The difference in phase precession between CA2 and CA3 did not reach statistical significance (Mann-Whitney *U*: CA2 vs. CA3, $z = 1.84$, $P = 0.066$) (Figure 2H–J and Table S2; see Figure S3 for examples of phase precession plots from individual CA2 fields).

After finding that CA2 cells had the basic firing characteristics of hippocampal place cells with only minor quantitative differences during single 10-min random foraging sessions, we asked whether CA2 ensembles exhibited additional population coding features that are typical of neural networks in CA1 and CA3 and next analyzed neuronal activity patterns during the four recording sessions within a block, two in a square enclosure and two in a circular enclosure (Figure 3A). As expected (Leutgeb et al., 2005; Lever et al., 2002; Muller and Kubie, 1987), the activity patterns of CA1 and CA3 cells were distinct between these contexts. However, the shape preference of CA2 cells was considerably lower than in the other CA regions (Mann-Whitney *U*: CA1 vs. CA2, $z = 7.59$, $P < 0.001$; CA1 vs. CA3, $z = 0.62$, $P = 0.54$; CA2 vs. CA3, $z = -4.53$, $P < 0.001$) (Figure 3B–C; see also Figure S4 for a description of the shape preference score accompanied by individual CA2 examples). Weak discrimination between spatial contexts by hippocampal network activity would typically be a result of unchanged network representations for different box shapes, but could also emerge when there is low baseline reproducibility of activity patterns for repetitions of the same shape. To distinguish between these alternatives, we computed population vector correlations between pairs of sessions (Figure 3D). We first tested whether spatial firing patterns were consistent between repeated visits to the same box shape. When selecting two consecutive sessions in the same box shape, CA2 showed activity patterns that were as consistent as in CA1 or CA3 [Mann-Whitney *U*: CA1 vs. CA2, $U(n1 = 7, n2 = 5) = 4$, $P = 0.091$; CA1 vs. CA3, $U(n1 = 7, n2 = 8) = 26$, $P = 0.87$; CA2 vs. CA3, $U(n1 = 5, n2 = 8) = 13$, $P = 0.71$] (Figure 3D–E). However, for repeated sessions in the same box shape that were separated by an intervening session of the other shape, CA2 was less consistent than CA1 or CA3 [Mann-Whitney *U*, CA1 vs. CA2, $U(n1 = 6, n2 = 4) = 1$, $P = 0.038$; CA1 vs. CA3, $U(n1 = 6, n2 = 4) = 0$, $P = 0.029$; CA2 vs. CA3, $U(n1 = 4, n2 = 4) = 0$, $P = 0.038$]. In fact, at this lag, the coding differences between repetitions of the same context were as pronounced as the coding differences between sessions in different contexts in CA2 [Mann-Whitney *U*: same shape vs different shape at lag 2, $U(n1 = 4, n2 = 8) = 10$, $P = 0.37$]. This suggests that any contextual coding that may be present in CA2 would be masked by temporal changes in network activity, even for intervals as short as 20 minutes.

To examine how time and contextual changes affect firing patterns in CA2 over longer time intervals, we analyzed the full experimental design in which rats randomly foraged in highly familiar environments in the morning and afternoon over 2 days (Figure 4A). The similarity between the CA2 population representations in identical enclosure shapes decreased monotonically as a function of the temporal distance between exposures for time intervals up to 18 h and then reached an asymptote of approximately 0.35 [ANOVA: $F(4) = 103.8$, $P < 0.001$; Tukey's HSD: all P-values < 0.001, except 18, 24, and 30 hour time points were not significantly different from each other]. The asymptotic value is larger than the correlation when cell identity was shuffled (> 99.9% of shuffled values for each time point were smaller than the mean of the actual values) (Figure 4B–C; see Figure S5 for timescales of up to 60 hours and Figure S6 for example cells from each rat). The time-dependent effect in CA2 was sufficiently pronounced that the amount of change due to time after six hours already exceeded the amount of change produced by distinct spatial contexts without a time lag (see Figure 4C). There were no circadian fluctuations in CA2 population similarity (Figure 4C) or in normalized firing rates (Figure S5), although there was a significant increase of firing rates within each recording block [two-way ANOVA: between blocks, $F(3) = 1.53$, $P = 0.21$; session number within blocks, $F(3) = 5.23$, $P = 0.0014$; Tukey's HSD between session 1 and session 4, $P < 0.01$; all other comparisons, n.s.].

Next, we compared the pattern of population similarity in CA2 with that of CA1 and CA3 in the same behavioral paradigm. The change in neuronal activity as a function of time was more pronounced in CA2 than in either the CA1 or CA3 cell populations [two-way ANOVA: brain region, $F(2) = 1061.1$, $P < 0.001$; time difference, $F(4) = 184.8$, $P < 0.001$; interaction, $F(8) = 24.6$, $P < 0.001$; Tukey's HSD between brain regions, $P < 0.001$]. We confirmed that the larger difference in firing patterns with time in CA2 compared to the other hippocampal subregions could not be attributed to the quality of the isolation of single units (Figure S1) and that it was found in all but one single rat (Figures S5 and S6). We also confirmed that the decrease in correlation over time was found irrespective of the number of intervening recording blocks (Figure S5). The passage of time rather than the amount of exposure to the recording environment therefore best explained the difference in the CA2 firing patterns. Finally, we calculated shape preference for each field across all 16 recording sessions, of which eight were in the square and eight were in the circular enclosure. CA2 showed much lower shape preferences than either CA1 or CA3 (Mann-Whitney U: CA1 vs. CA2, $z = 8.16$, $P < 0.001$; CA1 vs. CA3, $z = -0.23$, $P = 0.82$; CA2 vs. CA3, $z = -6.09$, $P < 0.001$), and the shape preference scores in CA2 were not significantly different than scores after randomly shuffling shape identity (only 67.9% of shuffled scores were lower than the actual mean score) (Figure 4D; see Figure S4 for individual examples). CA2 is therefore the only hippocampal subregion in which the population code more prominently differs between highly similar experiences at different time points than between different spatial contexts in close temporal proximity.

To determine whether the emergence of inconsistency in coding for the same box shape in CA2 required the intervening experience in a different box shape, we also performed recordings in a paradigm in which all 10-minute random foraging sessions were performed in the same box shape (n = 62 CA1 cells in 4 rats, 34 CA2 cells in 2 rats, and 70 CA3 cells

in 2 rats; Figure 5A–B, Table S1). In this paradigm, we found that the population vector correlation between sessions within a block was generally lower in CA2 than in the other subregions, but that the correlation decreased in all three hippocampal subregions with an increasing lag [Two-way ANOVA: brain region, $F(2) = 19.8$, $P < 0.001$; lag, $F(2) = 40.1$, $P < 0.001$; interaction, $F(4) = 1.73$; $P = 0.15$; Tukey's HSD between CA2 and CA1 and between CA2 and CA3, $P < 0.001$] (Figure 5C). The similar trend for CA1 and CA3 as for CA2 within a block of four recording sessions raised the question whether the more pronounced decline in CA2 compared to the other CA subregions, which we had observed in the two-shape paradigm, would at longer time intervals also emerge in the single-shape paradigm (Figure 6A). When comparing CA2 population vectors between blocks of recordings in a single shape, the similarity decreased as a function of the temporal distance between recording sessions for time intervals up to 18 h [ANOVA: $F(4) = 202.6$, $P < 0.001$; Tukey's HSD, P-values < 0.001 for all comparisons except comparisons between the 18, 24, and 30 hour time points were n.s.] (Figures 6B–D), and the decrease over time was more pronounced in CA2 than in either CA1 or CA3 [Two-way ANOVA: region, $F(2) = 1204.2$, $P < 0.001$; time difference, $F(4) = 263.5$, $P < 0.001$; interaction, $F(8) = 79.5$, $P < 0.001$; Tukey's HSD between brain regions, $P < 0.001$]. By charting the PV correlations between the first session of each block and all the other sessions within the two-day recording sequence, we could directly compare the population vector correlation within a block with the correlation between blocks (Figure S7). All CA subregions showed a short-term decrease in their correlation within a block. Between blocks, the correlation reset to a higher value in CA3 while it typically continued to decrease in CA2. CA1 was intermediate between CA2 and CA3. The recordings with only a single shape therefore confirmed that CA2 is the hippocampal subregion in which the change of the population code over time periods of hours is most pronounced.

Differences in the CA2 population code over time may result from various sources of variability in the firing patterns, such as from a loss or gain of firing fields, from a drift in place field location, or from rate changes within single firing fields. These possibilities can be distinguished by measuring the number and location of place fields over different time periods (Figure 7A). We compared the number of active firing fields of CA2 cells with those of CA1 and CA3 cells when averaging over an increasing number of sessions (i.e. one session, a block of four sessions, the eight sessions in a single day, and sixteen sessions over two days). CA1 and CA3 showed no difference in the number of fields over different time periods, whereas in CA2, the mean number of place fields per cell increased for increasingly longer analysis periods [Two-way ANOVA: brain region, $F(2) = 214.1$, $P < 0.001$; time scale, $F(3) = 13.7$, $P < 0.001$; interaction: $F(6) = 4.24$, $P < 0.001$; Tukey's HSD between brain regions, $P < 0.001$] (Figure 7B). Furthermore, we found that place fields from a single cell modulated their firing rates independently (Figure S8). Thus, the transient presence and independent modulation of each of the multiple firing fields of CA2 neurons is a source of the decorrelation within the CA2 network over time. In addition, changes in field locations could also cause decorrelation. To test this directly, we estimated the center of each place field in each session and traced the trajectory of the centers across the sixteen 10-min recording sessions in the single-shape experiment. CA2 place field centers drifted considerably more than those in CA1 and in CA3 (Mann-Whitney U: CA1 vs. CA2, z =

−4.61, $P < 0.001$; CA1 vs. CA3, $z = 1.74$, $P = 0.073$; CA2 vs. CA3, $z = 4.52$, $P < 0.001$) (Figure 7C). We therefore detected that both spatial drift and firing rate variability were much higher in CA2 than in the other subregions over long time intervals but not over short time intervals. These findings indicate that a combination of loss or gain of firing fields, changes in firing rate, and moderate drift in precise firing location of CA2 place cells resulted in the substantial change in neuronal activity patterns in the CA2 network over time.

Discussion

The distinct connectivity, gene expression profiles, and cellular plasticity of CA2 (Caruana et al., 2012; Chevaleyre and Siegelbaum, 2010; Cui et al., 2013; Hitti and Siegelbaum, 2014; Kohara et al., 2014; Lein et al., 2005; Pagani et al., 2014; Rowland et al., 2013; Woodhams et al., 1993; Zhao et al., 2007) suggest that its neuronal computations differ from the other hippocampal subregions. To test for specialized neural network activity, we recorded activity patterns from CA2 cells in behaving animals. We found that standard spatial and temporal firing patterns in CA2 at the level of single neurons, such as place fields, theta modulation, and phase precession, are comparable to the other CA fields, with only minor quantitative differences. This confirms a previous report in which differences in location-selective firing between CA2 and CA1 cells were not detected (Martig and Mizumori, 2011). However, when comparing activity patterns during repeated visits to the same environment over extended time periods, major differences in the CA2 firing patterns emerged. Rather than faithfully coding for features of an environment and for differences between environments, as is characteristic of CA1 and CA3, our data show pronounced variability in the spatial firing patterns of CA2 cells over hours and days. The major time dependent differences were a consequence of the fact that CA2 cells could exhibit place fields at multiple locations, of which only a subset was selectively active at any point in time. The firing rates within each of the fields of a CA2 cell varied independently, and each field showed drift around its central firing position. Through these combined changes in the firing patterns of each cell, the population coding of CA2 changed over time, and the amount of change after 6 hours already exceeded the amount of change as a consequence of presenting different environments. Together with behavioral evidence that neither silencing of CA2 nor ablating vasopressin 1b receptors, which are selectively enriched in CA2, impacts performance on spatial and contextual tasks (DeVito et al., 2009; Hitti and Siegelbaum, 2014), this suggests that CA2 is less specialized for representing space and for distinguishing between spatial contexts than the other hippocampal subfields.

The generation of distinct neuronal codes for different contexts is a prominent feature of hippocampal neuronal activity patterns in CA1 and CA3 (Anderson and Jeffery, 2003; Leutgeb et al., 2004; Lever et al., 2002; Muller and Kubie, 1987; Vazdarjanova and Guzowski, 2004). A study using immediate early gene labeling as a marker for neuronal activity in the mouse recently reported that the CA2 region is similar to CA1 and CA3 in that it generates distinct neural codes for two different environments that are presented with an interval of 20 minutes (Wintzer et al., 2014). At temporal distances on the order of minutes and without any intervening experiences, we also found that two different contexts resulted in a more distinct CA2 firing pattern than a repetition of the same context (see Figure 3E). However, when we extended our recordings to longer time intervals, the

changes in firing patterns with time were much more pronounced than the component of the decorrelation that was context dependent. These major changes over time rather than in response to distinct contexts are contrary to what we observed in the same paradigm in the CA1 and CA3 networks, where network similarity for repeated presentations of the same environment, even over intervals of 30 hours, is higher than for distinct contexts at close temporal proximity (Mankin et al., 2012; see also Figure 4C).

The lower stability of CA2 firing patterns could originate from the unique connectivity and physiology of this hippocampal subregion. For example, long-term potentiation (LTP) at the synapses between CA3 and CA2 is not inducible by standard protocols in hippocampal slices while these synapses can be potentiated by neuropeptides (Caruana et al., 2012; Chevaleyre and Siegelbaum, 2010; Pagani et al., 2014; Zhao et al., 2007). In CA1, pharmacological blockade of LTP reduces place field stability while conditions that enhance LTP result in more stable CA1 place fields (Kentros et al., 1998; Kentros et al., 2004). Thus, one source of place field instability in CA2 could potentially be the more limited LTP of inputs from CA3, and stability may increase by peptide release during behaviors that depend on vasopressin 1b receptor activation (DeVito et al., 2009; Pagani et al., 2014; Wersinger et al., 2002). However, it is currently unknown whether plasticity in CA2 can be modulated during behavior and, because CA3 inputs to CA2 are at baseline already weaker than entorhinal inputs (Chevaleyre and Siegelbaum, 2010), it is uncertain whether modulating plasticity at the CA3 inputs to CA2 would have major effects on CA2 firing patterns. Rather, from the findings that entorhinal inputs to CA2 are strong and that the resting membrane potential of CA2 cells is lower than in other hippocampal subregions (Chevaleyre and Siegelbaum, 2010; Zhao et al., 2007), it appears that CA2 activity may be more directly dependent on the convergence of inputs from entorhinal subdivisions. Medial entorhinal inputs to the hippocampus consist of grid cells, head direction cells, border cells, and nonspatial cells (Hafting et al., 2005; Sargolini et al., 2006; Zhang et al., 2013) while lateral entorhinal inputs are generally less modulated by spatial features than those from the medial entorhinal cortex (Deshmukh and Knierim, 2011; Hargreaves et al., 2005; Tsao et al., 2013). Furthermore, grid cells were found to not be context selective (Fyhn et al., 2007). Taken together, this raises the possibility that the reduced context selectivity and high variability of CA2 firing patterns results from the convergence of spatial and nonspatial entorhinal inputs, which have not been processed by the dentate gyrus and/or CA3. We also observed that CA2 cells can become silent within a particular firing field to only later reemerge at the same location. This observation suggests a stable spatial input over time from either the entorhinal cortex or, alternatively, from CA3, which has weaker input to CA2 (Chevaleyre and Siegelbaum, 2010) but has previously been found to retain consistent spatial representations in the same experimental paradigm (Mankin et al., 2012).

The observation that there is a strong time-varying signal in the CA2 network compared to other hippocampal subregions raises questions about the function of neuronal firing patterns that vary over time within a brain structure that is required for long-term memory. It has been found that noise or variability over time can be used as a neural coding mechanism. For example, a time-varying signal in memory circuitry has been shown to be necessary in brain circuits for motor learning (Stepanek and Doupe, 2010; Wu et al., 2014). Furthermore, findings in rats and human subjects demonstrate that a time-varying code in the

hippocampus and medial temporal lobe can predict subjective estimates of elapsed time, as well as performance on temporal order and sequence memory tasks (Ezzyat and Davachi, 2014; Hsieh et al., 2014; Manning et al., 2011; Manns et al., 2007). These experiments demonstrate that neural drift on a time scale of up to minutes is informative and that gradually changing activity patterns in the hippocampus can be integrated into a neural code that contains memory for temporal context. A particularly clear manifestation of a temporal code are the recently discovered sequence and time cells in the hippocampus, which fire in a stereotyped order while animals are stationary over periods of up to tens of seconds during each delay period (MacDonald et al., 2011; Pastalkova et al., 2008). Here we find a pronounced gradual change in CA2 ensemble activity over intervals of hours, but it remains to be determined whether neuronal firing patterns that fluctuate over this time scale could become repeated. Although there is no theoretical reason why temporal coding with repeated sequences would be limited to a particular time scale, it is likely that sequential neuronal activity on a much longer time scale would require different underlying cellular and circuit mechanisms than the sequential activation of CA1 cells over much shorter intervals. In contrast to a mechanism that relies on fixed sequences to be informative about elapsed time, it is also feasible that the time-varying neuronal firing patterns do not become informative by direct repetition during memory recall, but that it is rather a transition from changing to fixed neuronal firing patterns that supports memory, as has been suggested for neuronal activity in the mouse CA1 subregion (Kentros et al., 2004; Wang et al., 2012).

Alternatively, the CA2 cell population may contribute to memory coding neither by showing a sequence code nor by becoming stable, but by continuing to fluctuate and by thus providing a unique input pattern to CA1 at different time points. In this coding scheme, the variability over time in CA2 would be a prerequisite for providing temporal context, but it would not by itself constitute the temporal code. Rather, the unique inputs from CA2 would be associated with other stable inputs to CA1, such that CA1 activity patterns at one time differ somewhat from the activity patterns at a later time point. Such convergence of time-varying and stable inputs would provide a time-stamped neural code that differs between similar events at different times while it has higher overlap for events that occurred in close temporal proximity (Estes, 1955; Howard and Kahana, 2002; Mensink and Raaijmakers, 1988). In support of such combinatorial coding, the neural population code in CA1 has previously been identified to gradually vary over intervals of hours to weeks (Mankin et al., 2012; Manns et al., 2007; Ziv et al., 2013) while also faithfully continuing to discriminate between spatial contexts (Mankin et al., 2012). Yet it has not been apparent how reliable representations of different environments could be retained in CA1 while also allowing the network activity in the same cell population to drift over time. We now show that the dissimilarity in CA1 population activity over time is intermediate between CA2 and CA3, and it is known that CA1 receives strong excitatory inputs from both the CA3 and the CA2 subregion (Bartesaghi and Gessi, 2004; Bartesaghi et al., 2006; Chevaleyre and Siegelbaum, 2010; Kohara et al., 2014). This suggests that the CA1 network can integrate and/or compare the consistently precise information about spatial context it receives from CA3 with the slowly changing firing patterns we characterized in CA2 (Figure 8). The intermediate response of CA1 could thus indicate that the final processing stage of the hippocampus integrates information from not only CA3 and entorhinal cortex, but also from CA2 such

that the stability of the CA1 firing patterns is dynamically regulated to determine the persistence and temporal context of hippocampal memory signals.

Experimental Procedures

Subjects and surgical procedures

Eight male Long-Evans rats (400–510 g) were implanted with a multitetrode drive assembly ('hyperdrive') aimed at the right hippocampus (AP 3.9–4.0 mm posterior to bregma, ML 3.0–3.5 mm). Tetrodes were prepared as described previously (Leutgeb et al., 2007) and were placed in the hippocampal cell layer using techniques optimized for recording stability across days (Mankin et al., 2012).

Behavioral procedures

After one week of recovery from surgery, rats were partially food-deprived and trained to forage for randomly scattered cereal crumbs in an enclosure with walls that could be shaped either as a square (80 cm by 80 cm) or as a 16-sided polygon (50 cm radius; referred to as a 'circular enclosure'). Training was performed in two daily blocks. The first block started at approximately 9:00 am and the second block at approximately 3:00 pm. Rats were trained to run for four 10-minute sessions during each block, with two sessions in the square enclosure and two sessions in the circular enclosure, presented in random order. The recording phase of the experiment began after 9 to 20 days of behavioral training. Recordings were first conducted for 2 days in the standard training paradigm (referred to as two-shape, day 1 and day 2). Additionally, a subset of animals was tested in a paradigm in which all random foraging sessions were conducted in a single enclosure shape (single-shape, day 1 and day 2).

Cell-tracking

Because our study depended on tracking the same set of principal neurons over an extended time period, we developed a customized version of MClust (Redish, A.D., http://redishlab.neuroscience.umn.edu/MClust/MClust.html) with added functions that allowed for the comparison of the cluster boundaries of each cell throughout a series of recording sessions. Clusters that persisted in the same region of parameter space throughout two days were accepted as single cells for further analysis. Care was taken to accept only cells that could be precisely followed from the beginning to the end of the data analysis (Figure S1).

Data Analysis

For tracked cells, we calculated spatial maps and identified place fields. For each place cell and field, we determined standard characteristics (e.g., mean rate, peak rate, spatial information, phase precession), and we analyzed the firing during individual passes through the place field. From the firing rate distribution within the place field in each enclosure shape, we derived a shape preference score (see Figure S4). For the entire population of cells recorded in each subregion, we calculated all pairwise population vector correlations between 10-minute sessions, and grouped them by the elapsed time between sessions and by comparisons between either different shapes or the same shape.

Statistical Analysis

Comparisons between the firing characteristics of hippocampal subregions were performed using the Mann-Whitney *U* test. Holm-Bonferroni corrections for multiple comparisons were applied to the *P*-values. Comparisons between population vector correlations over different time intervals were performed using the Mann Whitney *U* test when there were two conditions and using ANOVA when there were three or more time intervals. If comparisons were between multiple time intervals as well as between brain regions, two-way ANOVA was used. Tukey's HSD method was used for all post-hoc comparisons.

Histology

Tetrode locations were confirmed postmortem in histological material. Immunostaining for α-actinin-2 (i.e., a CA2 marker) (Ratzliff and Soltesz, 2001; Wyszynski et al, 1998) and cresyl violet were used to determine whether the final recording site for each tetrode was in or near the principal cell layers of the CA3, CA2, or CA1 subregion (see Figure S2).

Detailed descriptions on cell tracking, data analysis, and histology can be found in the Supplemental Experimental Procedures.

Approvals

All experimental procedures were performed as approved by the Institutional Animal Care and Use Committee at the University of California, San Diego and according to National Institutes of Health and institutional guidelines.

Supplementary Material

Refer to Web version on PubMed Central for supplementary material.

Acknowledgements

We thank B. Slayyeh and M. Wong for technical assistance, and C. Varga and I. Soltesz for immunohistochemistry protocols. This research was supported by NIMH (1R01MH-100349), the Ray Thomas Edwards Foundation, Walter F. Heiligenberg Professorship, NSF/BMBF German-US collaboration (CRCNS-IIS-1010463), NIMH Training Grant (T32MH 020002-14), and Alberta Innovates - Health Solutions.

References

Anderson MI, Jeffery KJ. Heterogeneous modulation of place cell firing by changes in context. J Neurosci. 2003; 23:8827–8835. [PubMed: 14523083]

Bartesaghi R, Gessi T. Parallel activation of field CA2 and dentate gyrus by synaptically elicited perforant path volleys. Hippocampus. 2004; 14:948–963. [PubMed: 15390176]

Bartesaghi R, Migliore M, Gessi T. Input-output relations in the entorhinal cortex-dentate-hippocampal system: evidence for a non-linear transfer of signals. Neuroscience. 2006; 142:247–265. [PubMed: 16844310]

Caruana DA, Alexander GM, Dudek SM. New insights into the regulation of synaptic plasticity from an unexpected place: hippocampal area CA2. Learn Mem. 2012; 19:391–400. [PubMed: 22904370]

Chevaleyre V, Siegelbaum SA. Strong CA2 pyramidal neuron synapses define a powerful disynaptic cortico-hippocampal loop. Neuron. 2010; 66:560–572. [PubMed: 20510860]

Cui Z, Gerfen CR, Young WS 3rd. Hypothalamic and other connections with dorsal CA2 area of the mouse hippocampus. J Comp Neurol. 2013; 521:1844–1866. [PubMed: 23172108]

Deshmukh SS, Knierim JJ. Representation of non-spatial and spatial information in the lateral entorhinal cortex. Front Behav Neurosci. 2011; 5:69. [PubMed: 22065409]

DeVito LM, Konigsberg R, Lykken C, Sauvage M, Young WS 3rd, Eichenbaum H. Vasopressin 1b receptor knock-out impairs memory for temporal order. J Neurosci. 2009; 29:2676–2683. [PubMed: 19261862]

Estes WK. Statistical Theory of Spontaneous Recovery and Regression. Psychological Review. 1955; 62:145–154. [PubMed: 14371893]

Ezzyat Y, Davachi L. Similarity Breeds Proximity: Pattern Similarity within and across Contexts Is Related to Later Mnemonic Judgments of Temporal Proximity. Neuron. 2014; 81:1179–1189. [PubMed: 24607235]

Fyhn M, Hafting T, Treves A, Moser MB, Moser EI. Hippocampal remapping and grid realignment in entorhinal cortex. Nature. 2007; 446:190–194. [PubMed: 17322902]

Hafting T, Fyhn M, Molden S, Moser MB, Moser EI. Microstructure of a spatial map in the entorhinal cortex. Nature. 2005; 436:801–806. [PubMed: 15965463]

Hargreaves EL, Rao G, Lee I, Knierim JJ. Major dissociation between medial and lateral entorhinal input to dorsal hippocampus. Science. 2005; 308:1792–1794. [PubMed: 15961670]

Hitti FL, Siegelbaum SA. The hippocampal CA2 region is essential for social memory. Nature. 2014; 508:88–92. [PubMed: 24572357]

Howard MW, Kahana MJ. A distributed representation of temporal context. J Math Psychol. 2002; 46:269–299.

Hsieh LT, Gruber MJ, Jenkins LJ, Ranganath C. Hippocampal Activity Patterns Carry Information about Objects in Temporal Context. Neuron. 2014; 81:1165–1178. [PubMed: 24607234]

Jones MW, McHugh TJ. Updating hippocampal representations: CA2 joins the circuit. Trends Neurosci. 2011; 34:526–535. [PubMed: 21880379]

Kentros C, Hargreaves E, Hawkins RD, Kandel ER, Shapiro M, Muller RV. Abolition of long-term stability of new hippocampal place cell maps by NMDA receptor blockade. Science. 1998; 280:2121–2126. [PubMed: 9641919]

Kentros CG, Agnihotri NT, Streater S, Hawkins RD, Kandel ER. Increased attention to spatial context increases both place field stability and spatial memory. Neuron. 2004; 42:283–295. [PubMed: 15091343]

Kjonigsen LJ, Leergaard TB, Witter MP, Bjaalie JG. Digital atlas of anatomical subdivisions and boundaries of the rat hippocampal region. Front Neuroinform. 2011; 5:2. [PubMed: 21519393]

Kohara K, Pignatelli M, Rivest AJ, Jung HY, Kitamura T, Suh J, Frank D, Kajikawa K, Mise N, Obata Y, et al. Cell type-specific genetic and optogenetic tools reveal hippocampal CA2 circuits. Nat Neurosci. 2014; 17:269–279. [PubMed: 24336151]

Lee I, Yoganarasimha D, Rao G, Knierim JJ. Comparison of population coherence of place cells in hippocampal subfields CA1 and CA3. Nature. 2004; 430:456–459. [PubMed: 15229614]

Lein ES, Callaway EM, Albright TD, Gage FH. Redefining the boundaries of the hippocampal CA2 subfield in the mouse using gene expression and 3-dimensional reconstruction. J Comp Neurol. 2005; 485:1–10. [PubMed: 15776443]

Leutgeb JK, Leutgeb S, Moser MB, Moser EI. Pattern separation in the dentate gyrus and CA3 of the hippocampus. Science. 2007; 315:961–966. [PubMed: 17303747]

Leutgeb S, Leutgeb JK, Barnes CA, Moser EI, McNaughton BL, Moser MB. Independent codes for spatial and episodic memory in hippocampal neuronal ensembles. Science. 2005; 309:619–623. [PubMed: 16040709]

Leutgeb S, Leutgeb JK, Treves A, Moser MB, Moser EI. Distinct ensemble codes in hippocampal areas CA3 and CA1. Science. 2004; 305:1295–1298. [PubMed: 15272123]

Lever C, Wills T, Cacucci F, Burgess N, O'Keefe J. Long-term plasticity in hippocampal place-cell representation of environmental geometry. Nature. 2002; 416:90–94. [PubMed: 11882899]

Lorente de No R. Studies on the structure of the cerebral cortex. II. Continuation of the study of the ammonic system. J Psychol Neural. 1934; 46:113–117.

Ludvig N. Place cells can flexibly terminate and develop their spatial firing. A new theory for their function. Physiol Behav. 1999; 67:57–67. [PubMed: 10463629]

MacDonald CJ, Lepage KQ, Eden UT, Eichenbaum H. Hippocampal “time cells” bridge the gap in memory for discontiguous events. Neuron. 2011; 71:737–749. [PubMed: 21867888]

Magloczky Z, Acsady L, Freund TF. Principal cells are the postsynaptic targets of supramammillary afferents in the hippocampus of the rat. Hippocampus. 1994; 4:322–334. [PubMed: 7531093]

Mankin EA, Sparks FT, Slayyeh B, Sutherland RJ, Leutgeb S, Leutgeb JK. Neuronal code for extended time in the hippocampus. Proc Natl Acad Sci U S A. 2012; 109:19462–19467. [PubMed: 23132944]

Manning JR, Polyn SM, Baltuch GH, Litt B, Kahana MJ. Oscillatory patterns in temporal lobe reveal context reinstatement during memory search. Proc Natl Acad Sci U S A. 2011; 108:12893–12897. [PubMed: 21737744]

Manns JR, Howard MW, Eichenbaum H. Gradual changes in hippocampal activity support remembering the order of events. Neuron. 2007; 56:530–540. [PubMed: 17988635]

Marr D. Simple memory: a theory for archicortex. Philos Trans R Soc Lond B Biol Sci. 1971; 262:23–81. [PubMed: 4399412]

Martig AK, Mizumori SJ. Ventral tegmental area disruption selectively affects CA1/CA2 but not CA3 place fields during a differential reward working memory task. Hippocampus. 2011; 21:172–184. [PubMed: 20082295]

McNaughton BL, Morris RGM. Hippocampal Synaptic Enhancement and Information-Storage within a Distributed Memory System. Trends in Neurosciences. 1987; 10:408–415.

Mensink GJ, Raaijmakers JGW. A Model for Interference and Forgetting. Psychological Review. 1988; 95:434–455.

Muller RU, Kubie JL. The effects of changes in the environment on the spatial firing of hippocampal complex-spike cells. J Neurosci. 1987; 7:1951–1968. [PubMed: 3612226]

O'Keefe J, Recce ML. Phase relationship between hippocampal place units and the EEG theta rhythm. Hippocampus. 1993; 3:317–330. [PubMed: 8353611]

Pagani JH, Zhao M, Cui Z, Williams Avram SK, Caruana DA, Dudek SM, Young WS. Role of the vasopressin 1b receptor in rodent aggressive behavior and synaptic plasticity in hippocampal area CA2. Mol Psychiatry. 2014

Pan WX, McNaughton N. The supramammillary area: its organization, functions and relationship to the hippocampus. Prog Neurobiol. 2004; 74:127–166. [PubMed: 15556285]

Pastalkova E, Itskov V, Amarasingham A, Buzsaki G. Internally generated cell assembly sequences in the rat hippocampus. Science. 2008; 321:1322–1327. [PubMed: 18772431]

Ratzliff AD, Soltesz I. Differential immunoreactivity for alpha-actinin-2, an N-methyl-D-aspartate-receptor/actin binding protein, in hippocampal interneurons. Neuroscience. 2001; 103:337–349. [PubMed: 11246149]

Rolls, ET. Functions of neuronal networks in the hippocampus and cerebral cortex in memory. In: Cotterill, RMJ., editor. Models of brain function. Cambridge: Cambridge University Press; 1989. p. 15-33.

Rowland DC, Weible AP, Wickersham IR, Wu H, Mayford M, Witter MP, Kentros CG. Transgenically targeted rabies virus demonstrates a major monosynaptic projection from hippocampal area CA2 to medial entorhinal layer II neurons. J Neurosci. 2013; 33:14889–14898. [PubMed: 24027288]

Sargolini F, Fyhn M, Hafting T, McNaughton BL, Witter MP, Moser MB, Moser EI. Conjunctive representation of position, direction, and velocity in entorhinal cortex. Science. 2006; 312:758–762. [PubMed: 16675704]

Shen J, Barnes CA, McNaughton BL, Skaggs WE, Weaver KL. The effect of aging on experience-dependent plasticity of hippocampal place cells. J Neurosci. 1997; 17:6769–6782. [PubMed: 9254688]

Stepanek L, Doupe AJ. Activity in a cortical-basal ganglia circuit for song is required for social context-dependent vocal variability. J Neurophysiol. 2010; 104:2474–2486. [PubMed: 20884763]

Treves A, Rolls ET. Computational analysis of the role of the hippocampus in memory. Hippocampus. 1994; 4:374–391. [PubMed: 7842058]

Tsao A, Moser MB, Moser EI. Traces of experience in the lateral entorhinal cortex. Curr Biol. 2013; 23:399–405. [PubMed: 23434282]

Vazdarjanova A, Guzowski JF. Differences in hippocampal neuronal population responses to modifications of an environmental context: evidence for distinct, yet complementary, functions of CA3 and CA1 ensembles. J Neurosci. 2004; 24:6489–6496. [PubMed: 15269259]

Wang ME, Wann EG, Yuan RK, Ramos Alvarez MM, Stead SM, Muzzio IA. Long-term stabilization of place cell remapping produced by a fearful experience. J Neurosci. 2012; 32:15802–15814. [PubMed: 23136419]

Wersinger SR, Ginns EI, O'Carroll AM, Lolait SJ, Young WS 3rd. Vasopressin V1b receptor knockout reduces aggressive behavior in male mice. Mol Psychiatry. 2002; 7:975–984. [PubMed: 12399951]

Wintzer ME, Boehringer R, Polygalov D, McHugh TJ. The hippocampal CA2 ensemble is sensitive to contextual change. J Neurosci. 2014; 34:3056–3066. [PubMed: 24553945]

Witter MP. Intrinsic and extrinsic wiring of CA3: Indications for connectional heterogeneity. Learn Mem. 2007; 14:705–713. [PubMed: 18007015]

Woodhams PL, Celio MR, Ulfig N, Witter MP. Morphological and functional correlates of borders in the entorhinal cortex and hippocampus. Hippocampus 3 Spec No. 1993:303–311.

Wu HG, Miyamoto YR, Gonzalez Castro LN, Olveczky BP, Smith MA. Temporal structure of motor variability is dynamically regulated and predicts motor learning ability. Nat Neurosci. 2014; 17:312–321. [PubMed: 24413700]

Wyszynski M, Kharazia V, Shanghvi R, Rao A, Beggs AH, Craig AM, Weinberg R, Sheng M. Differential regional expression and ultrastructural localization of alpha-actinin-2, a putative NMDA receptor-anchoring protein, in rat brain. J Neurosci. 1998; 18:1383–1392. [PubMed: 9454847]

Young WS, Li J, Wersinger SR, Palkovits M. The vasopressin 1b receptor is prominent in the hippocampal area CA2 where it is unaffected by restraint stress or adrenalectomy. Neuroscience. 2006; 143:1031–1039. [PubMed: 17027167]

Zhang SJ, Ye J, Miao C, Tsao A, Cerniauskas I, Ledergerber D, Moser MB, Moser EI. Optogenetic dissection of entorhinal-hippocampal functional connectivity. Science. 2013; 340:1232627. [PubMed: 23559255]

Zhao M, Choi YS, Obrietan K, Dudek SM. Synaptic plasticity (and the lack thereof) in hippocampal CA2 neurons. J Neurosci. 2007; 27:12025–12032. [PubMed: 17978044]

Zhao X, Lein ES, He A, Smith SC, Aston C, Gage FH. Transcriptional profiling reveals strict boundaries between hippocampal subregions. J Comp Neurol. 2001; 441:187–196. [PubMed: 11745644]

Ziv Y, Burns LD, Cocker ED, Hamel EO, Ghosh KK, Kitch LJ, Gamal AE, Schnitzer MJ. Long-term dynamics of CA1 hippocampal place codes. Nat Neurosci. 2013; 16:264–266. [PubMed: 23396101]

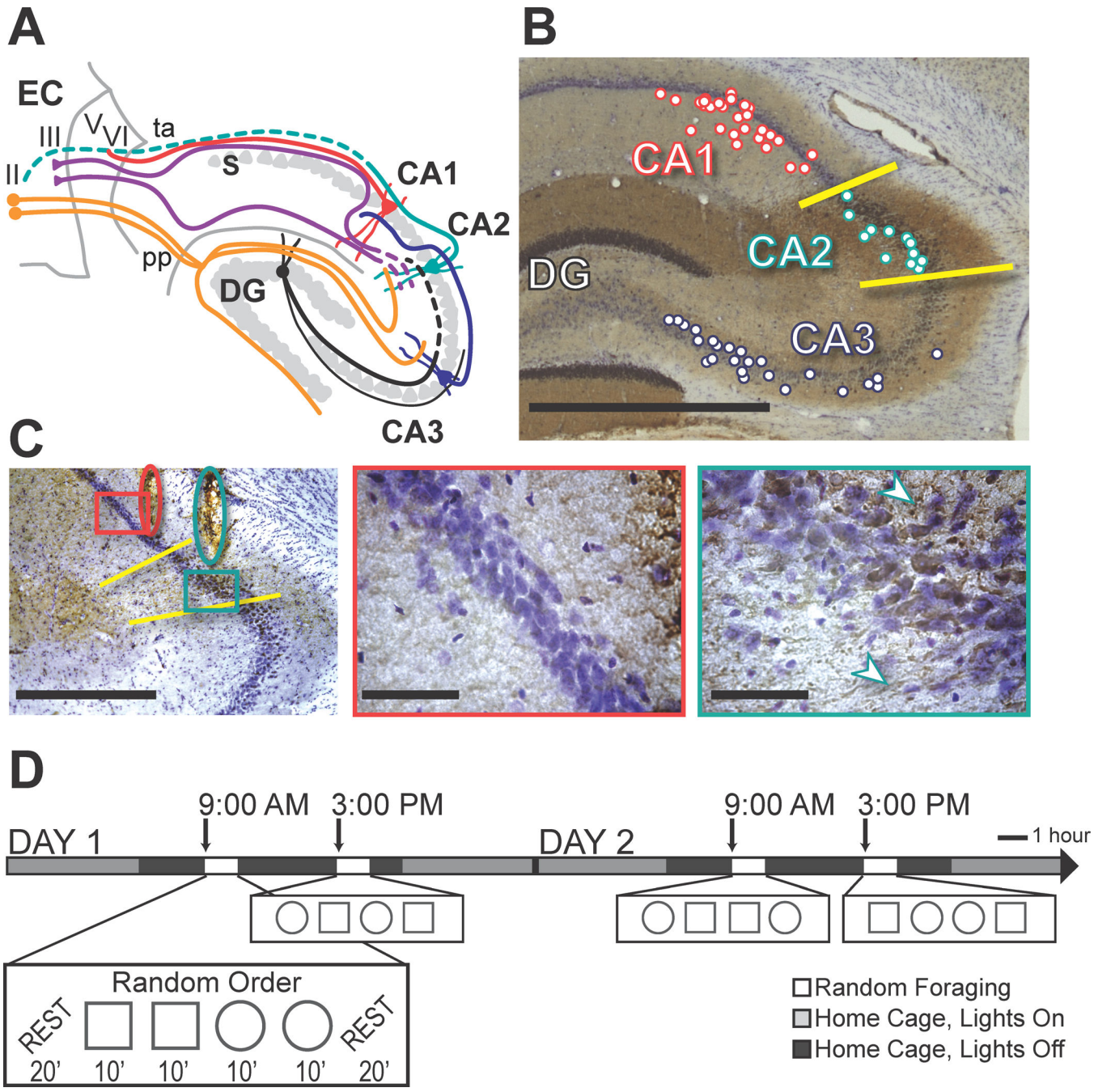

Figure 1.

Behavioral paradigm and the identification of recording sites in CA1, CA2, and CA3. (**A**) Schematic of the entorhino-hippocampal circuitry. Dotted lines denote CA2 connections that have recently been described but have not been confirmed in additional anatomical studies (Cui et al., 2013; Hitti and Siegelbaum, 2014; Kohara et al., 2014; Rowland et al., 2013). EC, entorhinal cortex; DG, dentate gyrus; S, subiculum; pp, perforant path; ta, temporoammonic path. (**B**) The hippocampal CA2 area (demarcated by yellow lines) is defined by positive α-actinin-2 immunoreactivity (brown), and cell bodies that are larger

and less densely packed than in CA1, as indicated with a cresyl violet counterstain (purple). The locations of all recording tetrode positions along the A–P axis are projected onto a representative section according to their proximal to distal position within each subregion, but note that tetrode placement spans up to 1 mm along the A–P axis. Tetrodes that were more anterolateral were targeted to either CA2 or CA3 while tetrodes that were more postermedial were targeted to CA1 or CA2. Because the orientation of the dorsal hippocampus is from anteromedial to posterolateral, this strategy resulted in electrode positions in CA1/CA2 and CA3 that were approximately matched for the longitudinal position within the hippocampus. Along the transverse axis, most recordings were in proximal CA1 while few recordings were in distal CA3 (i.e., close to CA2). Although this increased our confidence that CA3 recordings could not have been misassigned to CA2, this resulted in recording sites that were not precisely matched for connectivity between CA3 and CA1, which is strongest from distal CA3 to proximal CA1 (Witter, 2007). (**C**) Tetrode tracks in a section with α-actinin-2 and cresyl violet staining. Overview (left, scale bar = 500 μm) shows tetrode tracks (red oval, CA1; teal oval, CA2) with areas shown at high magnification to the right (red and teal boxes). In CA1 (middle), cell bodies are small, the cell layer is compact, and there is minor co-staining for α-actinin-2 (scale bar = 50 μm). In CA2 (right), cell bodies are larger and less densely packed, and there is strong α-actinin-2 staining in cell bodies and proximal dendrites (white arrowheads; scale bar = 50 μm). See Figure S2 for further illustration. (**D**) Behavioral design. A series of four 10-min random foraging sessions were performed in the morning and again in the afternoon, over multiple days. Each time block consisted of a random sequence of 2 sessions with the recording enclosure in a square configuration and 2 sessions in a circle configuration. Twenty-min rest sessions flanked the behavioral sequence. Single unit recordings commenced after 9–20 days of pretraining (‘Day 1’ indicates the first day of electrophysiological recording).

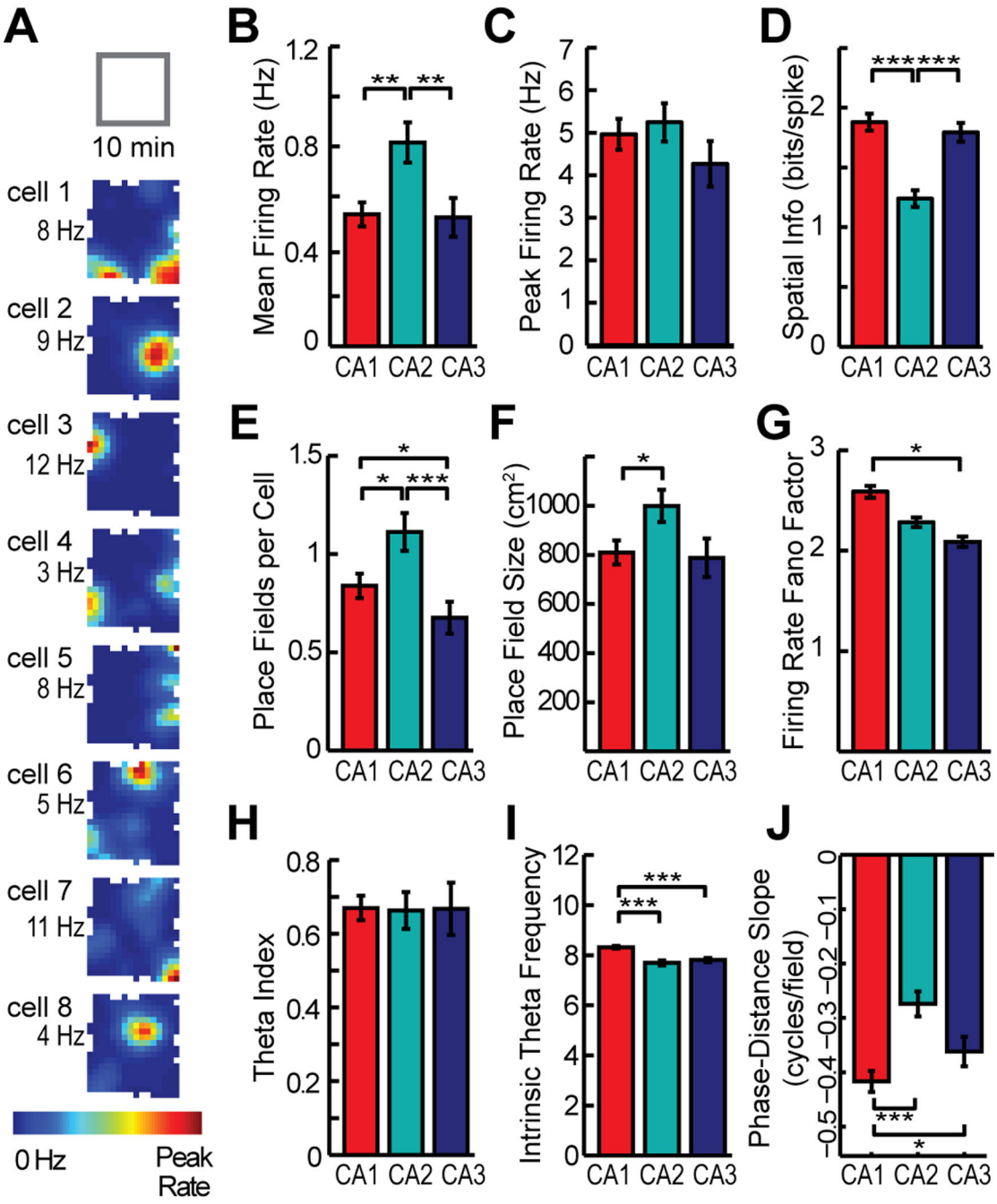

Figure 2.

The spatial and temporal firing patterns of individual hippocampal CA2 principal neurons in 10-min sessions are largely consistent with those of CA1 and CA3, but with quantitative differences. (**A**) The firing rate maps of eight CA2 cells that were recorded simultaneously during a 10-min random foraging session in a square-shaped box. Average firing rate in each spatial location is represented from 0 Hz (dark blue) to the peak rate for the cell (red, noted to the left of each map). (**B–F**) Rates were higher and spatial tuning in CA2 was broader than in CA1 and CA3. The broader spatial tuning resulted from an increase in place field

size and place field number per cell. (**G**) The variability in firing rate during individual passes through each place field did not differ between CA2 and the other CA subregions. (**H, I**) CA2 cells are modulated by the hippocampal theta rhythm to a similar extent as CA1 and CA2 cells and show intrinsic theta frequency comparable to CA3. (**J**) Place fields in CA2 showed phase precession, but to a lesser degree than in CA1. * $P < 0.05$, ** $P < 0.01$, *** $P < 0.001$ (Mann-Whitney U test). Bars are the mean ± SEM. See Table S2 and text for detailed statistics and Figure S3 for examples of phase precession.

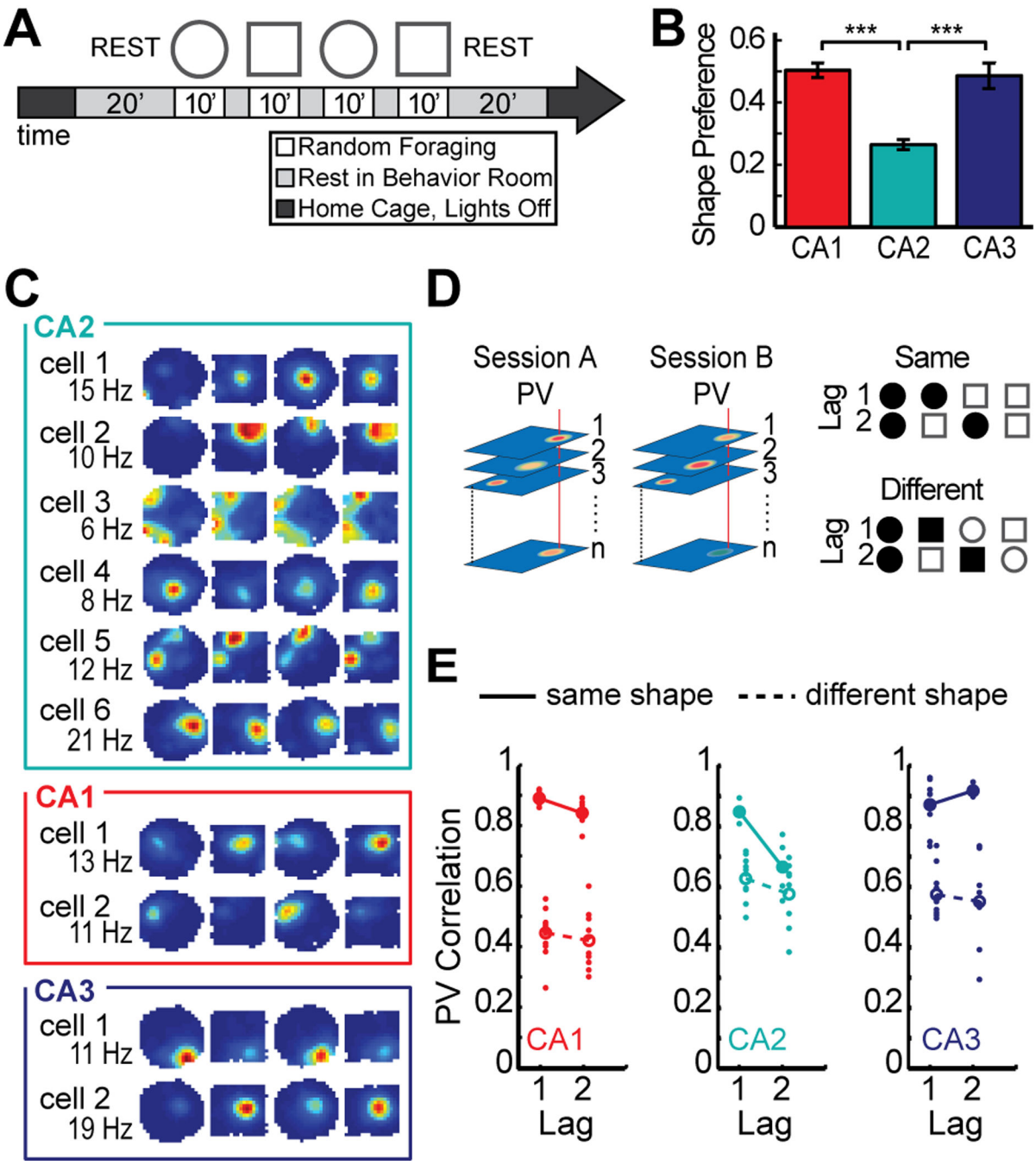

Figure 3.

Place fields in CA2 are weakly modulated by spatial context. (**A**) Experimental timeline. Four 10-min sessions of random foraging in a square and a circle-shaped box. (**B**) Place fields in CA2 had lower shape preference scores than fields in CA1 or CA3. See Figure S4 for a description of the shape preference score and individual examples. (**C**) Spatial firing rate maps for six representative CA2 cells and, for comparison, two CA1 cells and two CA3 cells. Maps are color coded as described in Figure 2A. CA2 cells 1–4 were recorded simultaneously with CA1 cells 1–2, and CA2 cells 5–6 were recorded simultaneously with

CA3 cells 1–2. The changes in the spatial firing patterns of CA2 cells were not correlated with the switching between box shapes. (**D**) The schematic on the left shows how population vectors (PVs) were calculated. The spatial maps of all cells in corresponding sessions were arranged into *x*–*y*–*z* stacks, where *x* and *y* represent the two spatial dimensions and *z* represents the cell identity. In each stack, the distribution of firing rates along the *z* axis for a given *x*–*y* location represents the population vector for that spatial bin (examples are denoted by the red vertical lines in each stack). To compare two recording sessions, the Pearson correlation coefficient was calculated between each pair of population vectors at corresponding locations, and the correlation coefficients of all spatial bins were averaged. A PV correlation of 1 indicates identical activity patterns and 0 indicates independent patterns. The schematic to the right gives examples of comparisons between pairs of sessions (filled shape symbols) for each time lag in either the same-shape or different-shape category. (**E**) Each pairwise population vector correlation is shown as a dot, and the mean correlation for each lag is shown as a circle (filled, same-shape; open, different-shape). These measures revealed that same-shape comparisons in CA2 were as stable as in CA1 or CA3 only for adjacent sessions (lag 1). *** $P < 0.001$. Symbols and error bars are the mean ± SEM.

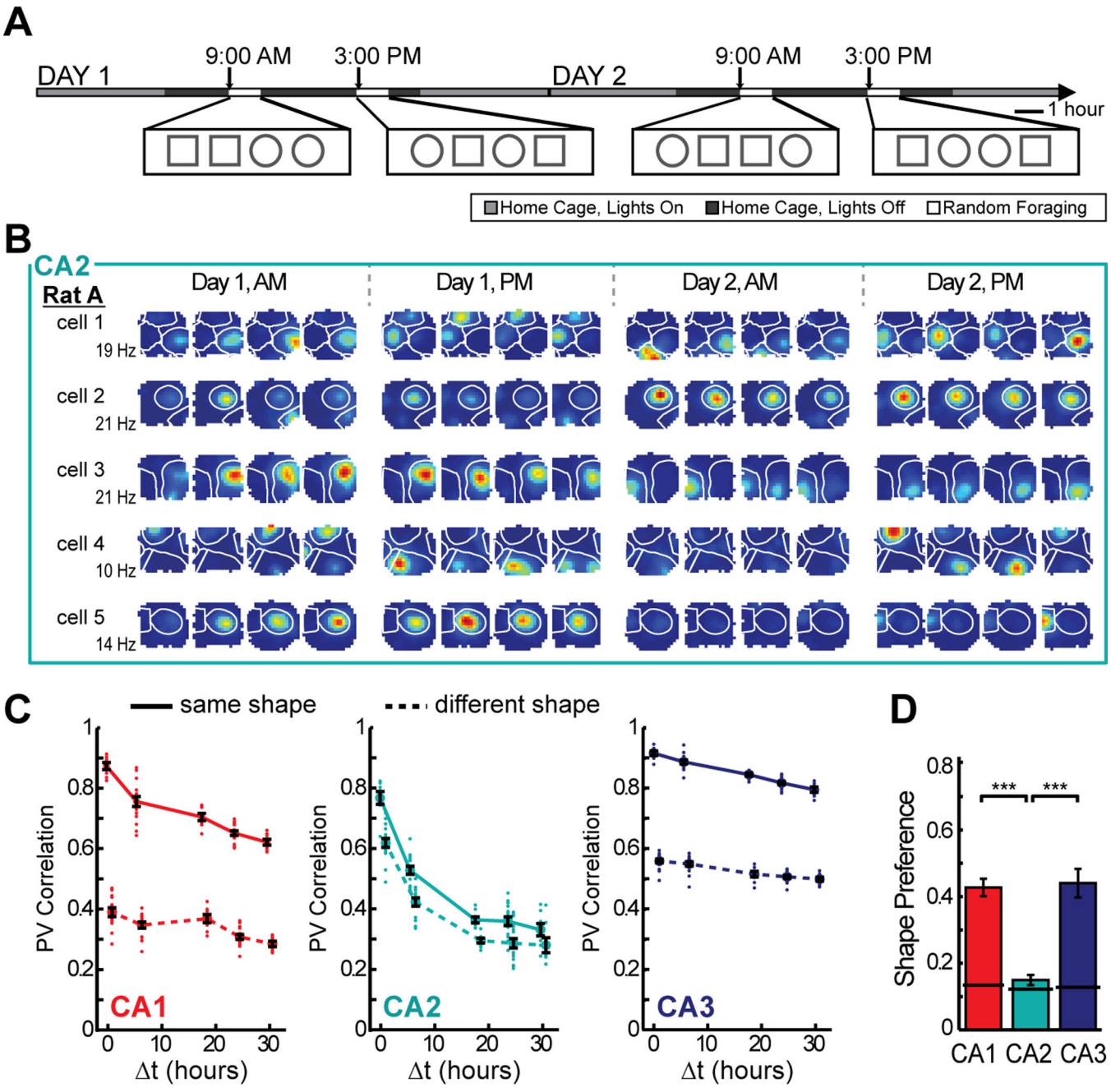

Figure 4.

Of the three hippocampal CA areas, CA2 is the only one that shows more pronounced change over time than between spatial contexts. (**A**) To examine the effect of temporal distance on spatial firing patterns in CA2, we recorded CA2 ensembles across two days during four blocks of four 10-min sessions. (**B**) Spatial firing rate maps for five simultaneously recorded CA2 cells. Place field boundaries, calculated from the average of the 16 spatial maps for each cell, are superimposed in white. Note that individual place fields can be off for several sessions before reappearing at the same location and that the firing rates of individual place fields from single cells are modulated independently (see

Figure S8). (**C**) The population vector correlation was calculated between pairs of sessions of either the same or different shape, and the comparisons were grouped by the time interval between sessions (Δt). Each dot represents a pairwise comparison, and symbols and error bars represent the mean +/− SEM for each time lag. The mean correlations for same shape comparisons are connected by a solid line, while the mean correlations for comparisons between square and circle are connected by a dotted line. (**D**) Place fields in CA2 had lower shape preference scores than fields in CA1 or CA3, and their scores were not different from a shuffled distribution across all 16 sessions (solid black line). See Table S3 and text for detailed statistics, Figure S1 for cluster stability, Figure S5 for additional analysis, and Figure S6 for examples from each rat. *** $P < 0.001$.

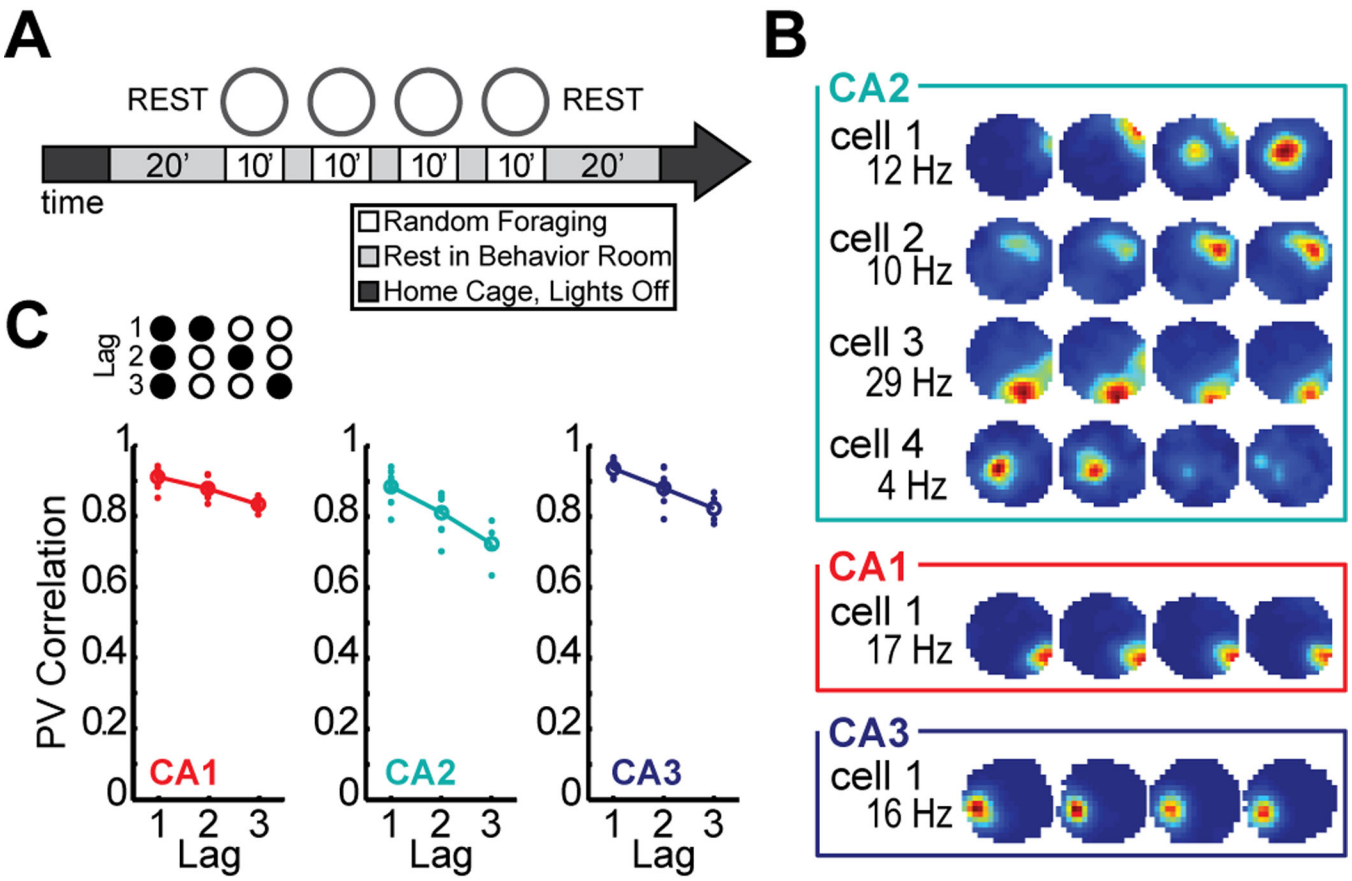

Figure 5.

In the single-shape paradigm all hippocampal subregions are characterized by a short-term decrease in the correlation of population activity. (**A**) To determine whether the inconsistency in coding for the same box shape in CA2 required the intervening experience in a different box shape, we performed recordings in a paradigm in which all 10-min random foraging sessions were in the same box shape. (**B**) Spatial firing rate maps for four representative CA2 cells are shown and, for comparison, one representative CA1 and CA3 cell. Maps are color coded as described in Figure 2A. Variability in spatial firing patters of CA2 cells occurred despite the consistent repetition of the same box shape over time. (**C**) An increase in the temporal distance between sessions within a block was accompanied by a decrease in the PV correlation in all three subregions, but the overall PV correlation was lowest in CA2. Symbols and error bars represent the mean +/− SEM for each time lag. See text for statistics and Figure S7 for additional analysis.

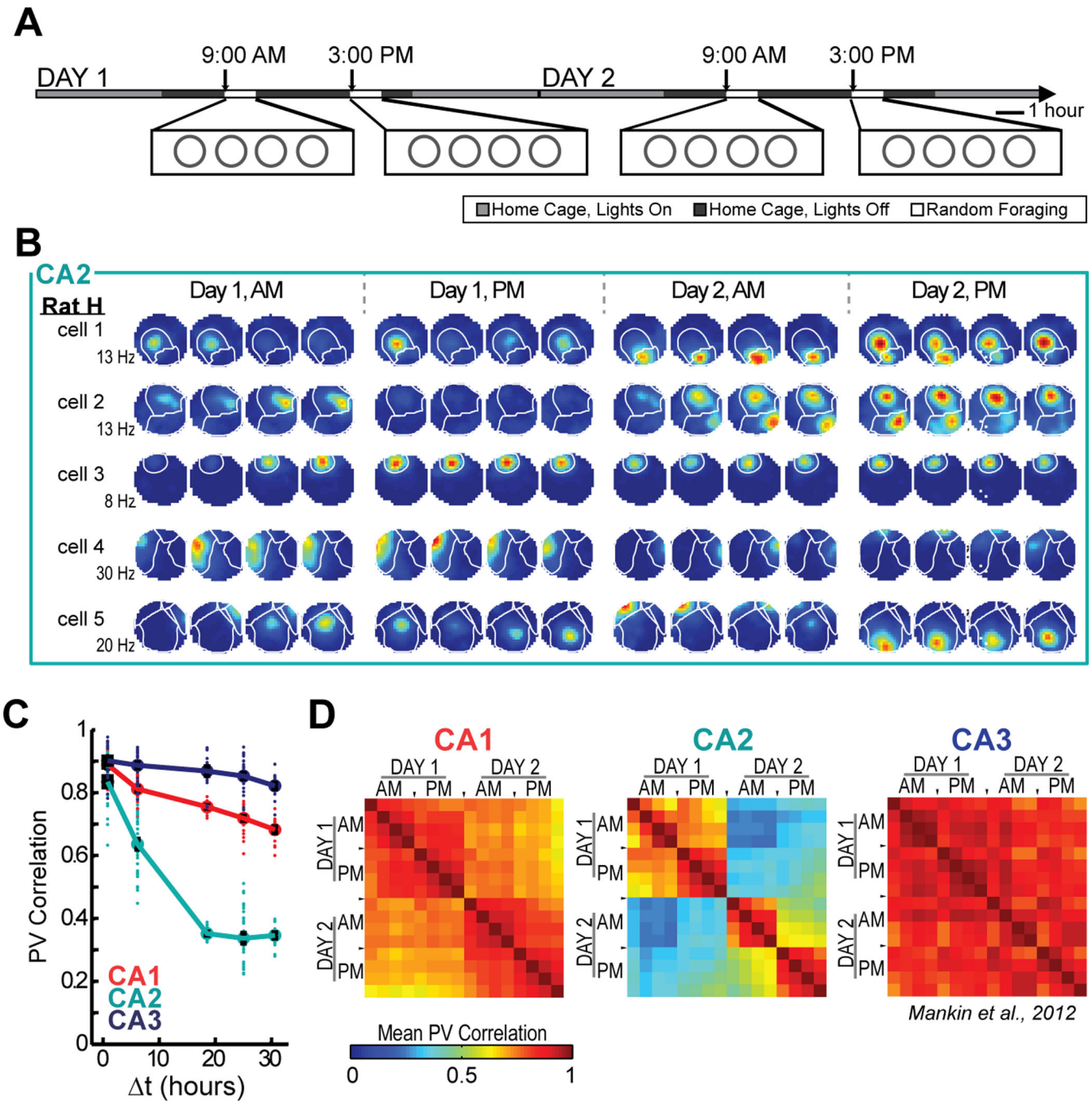

Figure 6.

The change in population activity over extended time periods was most pronounced in CA2 even when box shape was held constant. (**A**) To test whether the change in CA2 representations required two spatial contexts or would also be observed during testing in a single context, we recorded cells in only a single environment shape over two days. (**B**) Spatial firing rate maps for five simultaneously recorded cells in CA2 during the single-shape behavioral paradigm, with place field boundaries superimposed (white lines). As in the two-shape paradigm, place fields in CA2 cells appeared, vanished, and could reappear.

(**C**) In CA2, the decrease in PV correlation over time reached the same asymptotic level in the single-shape paradigm as in the two-shape paradigm, indicating that the change was predominantly a function of temporal distance and did not require switching between box shapes. In contrast, representations in CA3 have previously been shown to remain highly correlated over longer time intervals. In this paradigm, the CA2 and CA3 recordings are from different animals, and the CA3 recordings correspond to those reported in Mankin et al. (2012). Each dot is a pairwise comparison, and symbols and error bars represent the mean +/− SEM for each time interval. (**D**) Pairwise PV correlation matrices for repeated recordings in the same enclosure shape. Correlation matrices depict all possible comparisons between each of the sixteen recording sessions. Comparisons between the same sessions are shown along the diagonal, and their correlation coefficient is, by definition, 1. The lowest correlation coefficients were observed in the CA2 population for comparisons at intervals of at least 18 hours (see Figure S7 for additional plots).

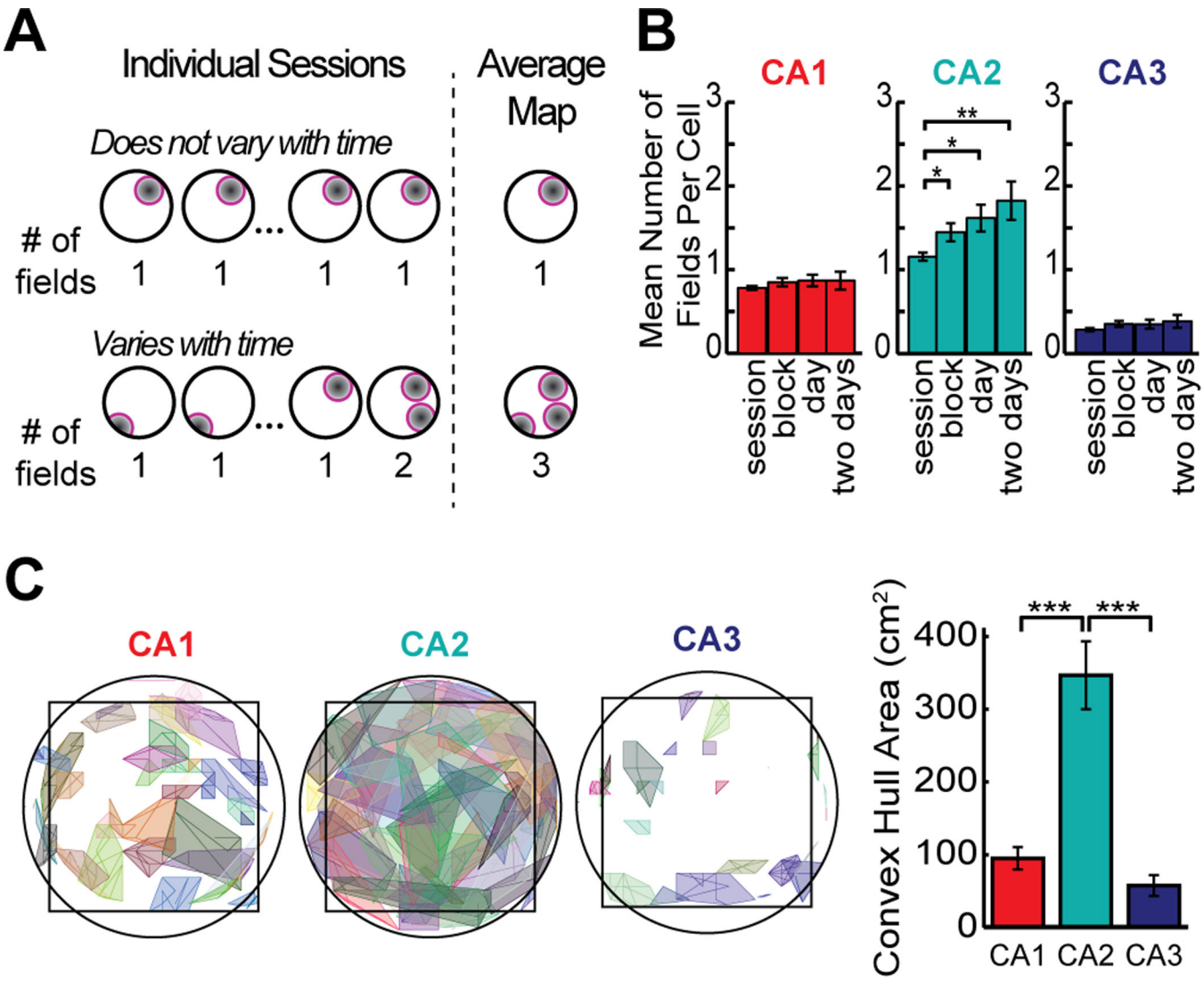

Figure 7.

Dissimilarity in spatial firing patterns in CA2 emerges from transiently silent firing fields accompanied by a drift in the center of each place field location. (**A**) The schematic shows that the number of fields in the average firing rate map remains constant over a series of sessions when cells have a consistent place field, but that the number increases when the firing rate switches on and off at multiple place field locations. See Figure S8 for additional analysis of firing rates. (**B**) Number of fields per cell in the single-shape paradigm after averaging over different time periods. In CA2, the number of fields per cell increased when including longer time periods, consistent with the idea that each cell can be transiently active at multiple firing locations (see Figures 4, 6, and S6 for examples). (**C**) To evaluate the degree to which firing within a place field was retained at a consistent location, place field boundaries were calculated from the average map (over 16 sessions). For each place field, the trajectory of the field center was then tracked across sessions, and the convex hull of the trajectory is shown. The bar graph to the right shows the average area of the fields' convex hulls, which was largest in CA2, indicating that the exact firing distribution within the field

varied from session to session. See text for detailed statistics. * $P < 0.05$, ** $P < 0.01$, *** $P < 0.001$. Bars represent the mean +/− SEM.

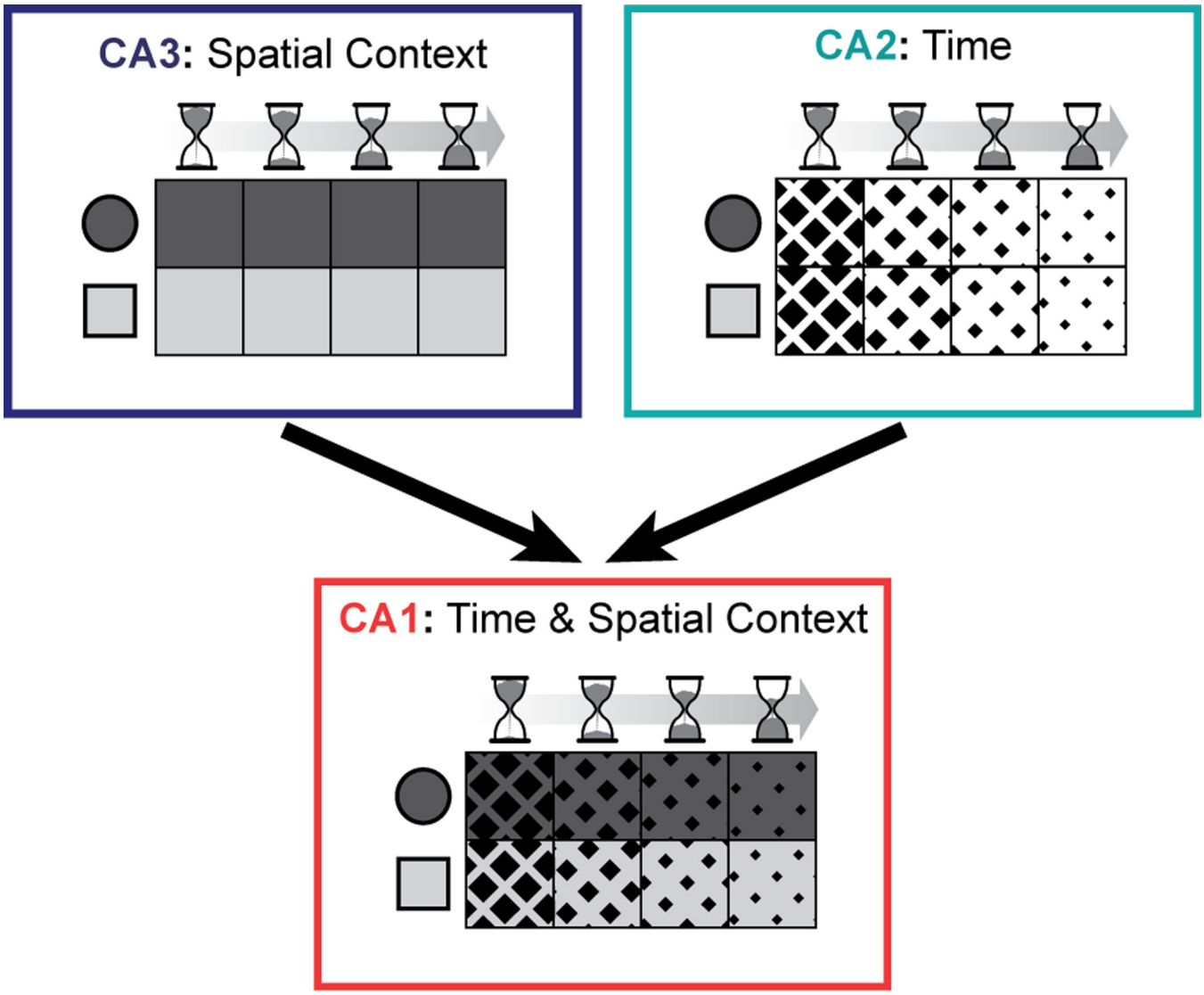

Figure 8.

A schematic of the coding in CA1, CA2, and CA3 for context and space at different times and how inputs from CA2 and CA3 could be combined to jointly reflect this information in CA1. The two-by-four grid for each hippocampal subregion depicts a population representation for events at different times (left to right) and in different spatial contexts (top and bottom). Firing patterns in CA3 differ depending on context (shades of gray) and firing patterns in CA2 differ depending on elapsed time (diamond size). CA1 shows coding for both aspects, possibly by integrating or comparing inputs from the other hippocampal subregions.